THIS IS AN ACCEPTED ARTICLE.

Polish Polar Research
DOI: 10.24425/ppr.2026.3127

This article has been accepted for publication in a future issue of *PPRes*, but has not been fully edited. Content may change prior to final publication.

Polluted fog can increase level of metal contamination in dwarf shrubs in High Arctic

Magdalena OPAŁA-OWCZAREK[1] ORCID-0000-0002-0583-6443, Mohit PHULARA[1] ORCID-0000-0002-1272-1476, Krzysztof SITKO[2] ORCID-0000-0002-4378-0399, Krzysztof MIGAŁA[3] ORCID-0000-0003-0881-8109, Wojciech SZYMAŃSKI[4] ORCID-0000-0002-5894-5176, Michał WĘGRZYN[5] ORCID-0000-0001-7638-4803, Bartosz KORABIEWSKI[3] ORCID-0000-0003-0824-0781 and Piotr OWCZAREK[3]* ORCID-0000-0001-7877-7731

[1] *Institute of Earth Sciences, University of Silesia in Katowice, Będzińska 60, 41-200 Sosnowiec, Poland*
[2] *Institute of Biology, Biotechnology and Environmental Protection, University of Silesia in Katowice, Jagiellońska 28, 40-032, Katowice, Poland*
[3] *Institute of Geography and Regional Development, University of Wroclaw, Plac Uniwersytecki 1, 50-137 Wrocław, Poland*
[4] *Institute of Geography and Spatial Management, Jagiellonian University, Gronostajowa 7, 30-387, Kraków, Poland*
[5] *Institute of Botany, Jagiellonian University, Gronostajowa 3, 30-387 Kraków, Poland*

***corresponding author:** piotr.owczarek@uwr.edu.pl

Received 2 February 2026 **Accepted** 31 July 2026

Running title: Polluted fog can increase metal contamination

Abstract: The impact of pollutants on plants and their spatial distribution, whether from distant locations or local sources, is not fully understood in the High Arctic. This is particularly relevant to the accumulation of pollutants in plants growing at different altitudes. This study aims to determine the concentration of metals in the area around Longyearbyen, which is Svalbard's largest emitter of pollutants, at different altitudes. Samples of polar willow, including both shoots and roots, were collected at three sites located at altitudes of 75–461 m a.s.l. Soil samples were also collected for testing to assess the chemical composition of topsoil and the concentration of exchangeable cations and plant-available elements. We analyzed the accumulation of Cd, Cu, Mg, Mn, Fe and Zn in bark and xylem. Our research indicates that pollutant levels in plants growing at altitudes of 420–461 m a.s.l. are *ca.* 2–3 times higher than in the valley. In addition, we found that the concentration of pollutants in the bark often exceeds > 10 times the values specified for wood, especially in the case of Fe, Mn and Zn. Dendrochronological studies confirm high concentrations of pollutants at higher altitudes. At polluted sites, the width of the growth rings was almost half that found in the less polluted valley. Plants at an altitude of > 420 meters are more frequently exposed to fog and low clouds, which directly supply them with polluted water.

Keywords: Arctic, Spitsbergen, metals, wet deposition, *Salix polaris*, dendrochronology.

Introduction

The High Arctic is among the most remote regions on Earth, yet it is increasingly affected by contaminants transported from lower latitudes via atmospheric and hydrologic pathways (Headley 1996; Bard 1999; Simões and Zagorodnov 2001). Long-range atmospheric transport (LRT) delivers metals such as Pb, Cd, Zn and Cu that are deposited onto snow, soils and vegetation across polar landscapes (AMAP 2015, 2021; Gworek *et al.* 2020). Increasing seasonal access has intensified human pressures, underscoring the need for sensitive, site-specific bioindicators (Anisimov *et al.* 2007; Afflerbach *et al.* 2017; Huntington *et al.* 2023). Most atmospheric pollution in the High Arctic originates from lower latitudes. These include volcanic emissions from Kamchatka, Alaska and Iceland, the mining and metallurgical industry on the Kola Peninsula and in the area of Norilsk (in eastern Siberia) and emissions from the oil industry and shipping (Law and Stohl 2007). Atmospheric circulation, which is controlled by conditions over the Norwegian Sea, Fennoscandia and Siberia, transports these pollutants towards the central parts of the Arctic Sea (Law and Stohl 2007; Stock *et al.* 2014; Nawrot *et al.* 2016). Depending on how pollutants are transferred to the environment, deposition can be classified as dry, wet, or fog. Direct deposition of fog to vegetation is particularly efficient in low clouds with bases below the level of plateaus and ridges (Myśkow *et al.* 2019).

Svalbard, especially the vicinity of Longyearbyen, exemplifies the combined influence of LRT and local sources (Zaborska *et al.* 2017; Rudnicka-Kępa and Zaborska 2021). Winter circulation frequently advects anthropogenic pollution from Europe and Russia, elevating aerosol and trace-element loads over the archipelago (Drbal *et al.* 1992; Birks *et al.* 2004). Superimposed on this background are emissions from energy production, vehicular traffic, a century of coal mining, and resuspension of coal-rich dust, producing spatially heterogeneous contamination around the settlement (Jóźwik 2000). After deposition, metals may be re-emitted, immobilized in soils or assimilated by plants. Approximately 90% of terrestrial Hg is sequestered by vegetation, whereas Cd and Pb are taken up mainly through roots, with foliar interception important near sources (Ismael *et al.* 2019; Schaefer *et al.* 2020; Zhou *et al.* 2021). Cryptogams (mosses, lichens) efficiently intercept atmospheric metals and are widely used as bioindicators (Grodzińska and Godzik 1991; Bargagli 2016; Wojtuń *et al.* 2018; Dziurowicz *et al.* 2025). Around Longyearbyen, elevated Pb, Cd, Cu and Zn in cryptogams and surface soils generally decline with distance and elevation from sources (Łokas *et al.* 2019), but such surveys reveal little about root-mediated uptake or longer-term internal storage in vascular plants (Saarela *et al.* 2005; Cocozza *et al.* 2016; Martin *et al.* 2018).

Tree-based studies clarify how different tissues register pollution: wood and growth rings can reflect the temporal evolution of heavy-metal availability, while bark directly receives atmospheric deposition on its outer surface (Sawidis *et al.* 2011; Chiarantini *et al.* 2016; Martin *et al.* 2018). The precise pathways into annual rings remain debated, and reconstructing histories from bark is complex (Rodríguez Martín *et al.* 2014; Chiarantini *et al.* 2016). Nonetheless, organ-resolved analyses, including paired bark/wood, help separate depositional from internal signals (Saarela *et al.* 2005). These lessons motivate a shrub-based approach for Svalbard. *Salix polaris* Wahlenb., a common and abundant plant around Longyearbyen, bridges soil and atmosphere; bark is a near-surface interface sensitive to recent deposition, whereas xylem wood integrates medium- to long-term internal accumulation and translocation, enabling a tissue-resolved view of exposure pathways in a treeless landscape (Martin *et al.* 2017; Myers-Smith *et al.* 2020; Owczarek *et al.* 2021).

Local context further supports this focus. Longyearbyen, having *ca.* 2200 residents, has a coal/diesel power plant, intense seasonal transportation, and a long coal mining legacy, as well as extensive abandoned infrastructure. Weathering and thaw of waste-rock piles and mine areas generate leachates and acid mine drainage, while windborne coal particles disperse broadly signals that are detected in soils, snow and aerosols near infrastructure (Cecinato *et al.* 2000; Rodríguez Martín *et al.* 2014; Weinbruch *et al.* 2015; Chiarantini *et al.* 2016; Gallet *et al.* 2019). Moreover, the altitudinal variation modulates exposure by affecting snow distribution, soil moisture, permafrost dynamics and vegetation structure. Although metals in cryptogams and soils generally decline with elevation and distance from sources, it remains unclear whether similar gradients occur in *S. polaris* tissues across Longyearbyen's topography (Łokas *et al.* 2019).

Accordingly, we quantify Cd, Zn, Cu, Fe, Mg and Mn in the bark and xylem wood of *S. polaris* from three altitudinal sites around Longyearbyen. For the first time in the Arctic, we investigate the relationship between pollutants accumulated in plants growing in a vertical gradient and dendrochronological data. Our main objectives are to (*i*) resolve spatial trends in tissue metal loads across sites, (*ii*) contrast bark, as the interface with recent deposition, with wood, as an integrator of medium- to long-term internal accumulation, and (*iii*) assess the impact of altitude on the distribution of pollution, especially the impact of polluted fog.

Study area

The study was carried out in the central part of Spitsbergen, the largest island in the High Arctic Svalbard archipelago (Fig. 1A). The landscape of this part of Spitsbergen is mainly characterized by wide plateau at an elevation 420–550 m a.s.l., above which single peaks and mountains rise to up to 1050 m a.s.l. (Fig. 1B). This type of relief is closely related to the geological structure, which consists of near-horizontal layers of sandstones, siltstones, and shales from the lower Cretaceous and lower Tertiary (Hjelle 1993). The elevated plateaus are often covered by rock debris with frost-patterned ground (Fig. 1B). In contrast, more profound erosional processes give rise to U-shaped valleys with extensive braided river systems and alluvial cones (Fig. 1C). There are small glaciers in the upper parts of the valleys and cirques, which have been rapidly retreating since the late 20th century (Małecki 2016). The study area is characterized by prevalence of Turbic Cryosols and Haplic Cryosols in the river valleys, whereas Skeletic Cryosols and Turbic Cryosols are the most common soils in the mountains (Szymański *et al.* 2022a, 2022b; Bartos *et al.* 2023). The soils show loamy texture and acidic reaction as well as various content of organic matter due to heterogeneous environmental conditions such as vegetation cover, soil wetness, and microclimate (Szymański *et al.* 2022a, 2022b; Bartos *et al.* 2023, 2024).

According to Köppen's system, the climate represents the tundra polar subtype (ET), with the average annual air temperature of –4.5°C and seasonal air temperatures varying between 11.7°C in winter and 5.2°C in summer. Compared to other parts of Spitsbergen, this area receives very low annual precipitation of 207.9 mm. Within plateaus, the dominant vegetation type is tundra classified as cryptogam, herb barren. This habitat is characterized by dry to wet barren landscapes with very sparse, extremely low-growing plant cover. Prostrate shrubs < 5 cm tall, such as *Dryas octopetala* and *Salix polaris*, along with graminoids and forbs, dominate in lower elevations and valleys.

The research sites are located near Longyearbyen (Fig. 1A), which is the largest settlement in Svalbard. Although its pollution level is generally low, it has numerous pollution sources. These are a coal and diesel fuel power plant and transportation, *e.g.*, snowmobiles, passenger cars, heavy-duty vehicles, vessels, and aeroplanes. Coal mining in the Longyearbyen area began in 1906, and seven mines were established. Although the last one was closed on 30 June 2025, the remains of the mines and industrial waste dumps accumulated over decades still exist and continue to have a negative impact on the environment (Askaer *et al.* 2008). To determine the impact of altitude on the accumulation of pollutants in plants, sites located on a plateau at an altitude of > 400 m a.s.l. (LYR 3: 420 m a.s.l., LYR 4: 461 m a.sl.) (Fig. 1B) and site located in the valley, in proximity to the settlement (LYR 8: 75 m a.s.l.) (Fig. 1C), were selected.

Materials and Methods

Plant material, sampling and analysis

For each study site established at the *Salix polaris* sampling locations, vegetation communities were characterized using phytosociological relevés, each covering an area of 100 m². Relevé locations were selected following the cardinal principle of identifying uniform and homogeneous plant community surfaces, as described by Braun-Blanquet (1964). *Salix polaris* (Wahlenb.), known as Polar willow, is widespread in the Svalbard archipelago, notably within south-western Spitsbergen and Edgeøya (Elvebakk 1994, 1997; Rønning 1996). Its prevalent distribution across Spitsbergen makes it a bioindicator species of environmental change, both natural and anthropogenic (Buchwal *et al.* 2013; Owczarek *et al.* 2013, 2014 Opala-Owczarek *et al.* 2018; Wojtuń *et al.* 2019). *Salix polaris* has a dense network of roots and woody shoots, although dark green leaves are usually visible on the surface (Fig. 2A). The woody part of the plant, where measurable annual growth rings with clear boundaries are visible, is surrounded by thick bark that protects it from extreme environmental conditions (Fig. 2B).

Samples of *S. polaris* were collected during two field campaigns, 2022 and 2023, from three sites: one at a low elevation in Longyeardalen Valley (LYR 8), and two on the Platåberget (Sverdruphamaren) plateau at an elevation of 420–461 m a.s.l. (LYR 3 and LYR 4). At every site, we randomly collected 15–20 individuals, depending on the availability in a given location.

The specimens were analyzed in the laboratory in two ways: dendrochronologically, to determine the characteristics of plant growth, and for metal content. For dendrochronological analysis, we adapted well-established microscopic techniques for dwarf shrubs (Gärtner and Schweingruber 2013). We carefully selected undamaged sections from each plant's main root and shoots. These samples were then rehydrated and thinly sliced to a 15–20 µm thickness, using a GSL 1 sledge microtome (Gärtner *et al.* 2014). Serial sectioning (Kolishchuk 1990; Myers-Smith *et al.* 2015) allowed for a detailed examination across various parts of each plant, addressing any absent or compressed rings. To measure growth rings, we captured digital photographs of each micro-section under 10x magnification, or 20x magnification for less regular samples. Given the prevalence of wedging and partially missing rings related to eccentric growth, at least two radii were measured under visual control using the WinDENDRO tree-ring system (Rinn 2003), ensuring accuracy in our analysis of growth-ring variability. We conducted cross-dating in three stages: first, among all measurements within each cross-section; next, among all measurements within each plant; and final, across the results from every site. The constructed chronologies were statistically verified in the program COFECHA (Grissino-Mayer 2001). Following this, the TRW series were standardized with the ARSTAN software (Cook and Holmes 1996) using a straight line with a horizontal slope, as no distinct age trend was revealed in the analyzed specimens.

Wood and bark samples of *S. polaris* were separated and washed prior to drying, packed into paper envelopes, and dried at 70°C for three days in a drier (WGLL-65BE, ChemLand, Poland). After drying, the samples were weighed using the same analytical balance. The dry wood and bark material was ground in a mortar, homogenized, and acid-digested in a microwave-assisted wet digestion system (ETHOS1, Milestone, Italy). The digestion protocol was developed for this study, taking into account the longer mineralization time required for woody tissue compared with typical herbaceous plant material, and used concentrated HNO_3 (65%, suprapure grade; Carlo Erba, Italy) and H_2O_2 (30%; Stanlab, Poland) in a 4:1 (v/v) ratio. Metal concentrations in the digests were determined by flame atomic absorption spectrophotometry (iCE 3500 FAAS; Thermo Scientific, USA). Reference plant material (Oriental Basma Tobacco Leaves [INCT-OBTL-5]; Institute of Nuclear Chemistry and Technology) was used to ensure analytical quality control. The results are shown as the means ± SE. To enable comparison of the significance of differences between examined *Salix polaris* populations in element concentration, a one-way ANOVA and a post hoc Fisher LSD test was used ($p < 0.05$). The statistical analysis was performed using Statistica v.13.1 software (Dell Inc., Austin, TX, USA).

Soil sampling and analysis

Soil samples were collected from the 0–10 cm surface layer to plastic bags and transported to the laboratory. In the laboratory, the samples were air dried at 22°C, gently crushed, and passed through a 2 mm stainless steel sieve. All living roots were removed from the soil samples. All soil analyses were performed using a fine-earth material, *i.e.*, fraction < 2 mm. Particle-size distribution was determined using a hydrometer method (silt and clay fractions) and sieving (sand fraction) according to Gee and Bauder (1986). Soil pH was measured potentiometrically in deionized water (1:2.5 w/v ratio) using a glass electrode (Thomas 1996). Content of total carbon (TC) and total nitrogen (TN) was determined in triplicate and then averaged, using a Vario Micro Cube CHN elemental analyzer (Vario Micro Cube, Elementar, Hanau, Germany). The content of TC was assumed as soil organic carbon content (SOC) due to the fact that all studied soil samples did not contain carbonates. The chemical composition of fine earth material (< 2 mm) was determined using Inductively Coupled Plasma-Emission Spectrometry (ICP-ES) at a certified laboratory of Bureau Veritas (Vancouver, BC, Canada). Concentration of exchangeable alkaline cations (Ca^{2+}, Mg^{2+}, K^{+} and Na^{+}) was measured using Flame Atomic Absorption Spectrometry (FAAS) after extraction with 1M ammonium acetate at pH = 7 (Sumner and Miller 1996). Concentration of exchangeable acidic cations H^{+} and Al^{3+} extracted using 1M KCl was determined by titration of extracts, after boiling for 10 s, with 0.1 M NaOH in the presence of phenolphthalein (Summer 1992). The colorimetric method (Kuo 1996) and FAAS were used to determine concentration of plant available phosphorus (Pav) and potassium (Kav), respectively. Concentration of plant available magnesium (Mgav) was measured by FAAS after extraction procedure according to Schachtschabel (1954). Determination of exchangeable alkaline (Ca^{2+}, Mg^{2+}, K^{+}, and Na^{+}) and acidic (H^{+} and Al^{3+}) cations as well as plant available elements (Pav, Kav, Mgav) concentration was done in certified laboratory of Bureau of Forest Management and Geodesy in Kraków.

Quality control for ICP-OES was ensured by the certified laboratory's internal protocols (ISO 17025 compliant). For FAAS (iCE 3500, Thermo Scientific), the limits of quantification (LOQ) were established based on 10 times the standard deviation of blank measurements. The precision of the method was monitored by analyzing samples in triplicate, with relative standard deviations (RSD) consistently < 5%. Linearity was maintained by keeping the absorbance values within the 0.05–0.5 range.

Results

Vegetation characteristics

To properly assess the variability in contaminant levels, we had to conduct a detailed analysis of the plant communities. The research sites are located in phytosociologically diverse areas, including a flat, rocky plateau Platåberget (LYR 3 and LYR 4), and the lower part of the slope of Gruvefjellet in the Longyeardalen valley (LYR 8). Platåberget is characterised by > 80% cryptogam dominance, with *Umbilicaria hyperborea, Rhizocarpon geographicum, Lecanora polytropa* and *Pseudephebe pubescens* forming continuous crusts or mats. Vascular plants, like *Salix polaris*, appear only as scattered stress-tolerant individuals. Such composition corresponds with descriptions of cryptogam-dominated polar desert terrains across Svalbard and other High Arctic archipelagos, where extreme abiotic stress results in vegetation physiognomy governed almost entirely by lichens and bryophytes (Rønning 1996; Węgrzyn and Wietrzyk 2015). The association develops on steep, wind-exposed slopes, blockfields and frost-shattered ridges, where soil formation is nearly absent. These features correspond directly to the polar desert ecotone described for the highest and driest surfaces of the central Spitsbergen landscape, which represents extremely poorly developed High Arctic fellfield vegetation (Elvebakk 2005). The lower parts of the slopes in the valley area, in contrast, have significantly greater biodiversity. This community is characterised by the co-dominance of evergreen dwarf shrubs (*Cassiope tetragona*), hemiprostrate shrubs (*Dryas octopetala*, *Salix polaris*), and a dense field layer of arctic herbs and graminoids. The presence of a continuous soil layer enables higher productivity and greater vegetation height compared to fellfields. Bryophytes and lichens remain abundant but clearly subordinate. These floristic and structural features reflect classic mesic tundra ecosystems on Svalbard with moderate moisture and improved nutrient cycling (Elvebakk and Prestrud 1996; Walker *et al.* 2005). The floristic composition of the sites within the valley is typical of stable, moist slopes and mesic tundra patches in the Longyearbyen area. It corresponds to the well-known shift from cryptogam-dominated to vascular-dominated vegetation under improved soil and moisture conditions (Węgrzyn and Wietrzyk 2015). Based on research by Wojtuń *et al.* (2019), vegetation in the valley floor near Longyearbyen is a bioindicator of trace element pollution. Increased metal content was found in *Sanionia uncinata* and *Salix polaris*, and it was pointed to as local contamination sources, such as exhaust from power plants, traffic, coal mines, and industrial waste dumps. However, for comparison purposes, samples from upland areas were not analysed.

Variation in metal content in plants *vs.* growth response

Analyses of metal concentrations revealed significant variations depending on the location of the site and the type of material being investigated (Fig. 3). In the wood of *S. polaris*, concentrations of the macronutrient Mg were consistently higher than those of the micronutrients Fe, Mn, and Zn at all tested fields and in both shoots and roots. Across sites LYR 3, LYR 4, and LYR 8, Mg ranged from *ca.* 530 to 3330 µg g DW. A translocation factor > 1 was observed only for site LYR 4. For the remaining sites, Mg accumulation in shoots was significantly lower than in root wood. In the case of Cd, Mn, and Zn, no significant differences were found between the accumulation in the wood of willow shoots and roots from sites LYR 3 and LYR 4. However, the highest Cd content was found in the wood of *S. polaris* shoots from LYR 3 among all the wood samples tested. The shoot wood from LYR 8 was characterized by the lowest accumulation of Cd, Cu, Mg, Mn, and Zn, and at the same time, it had the significantly highest Fe content among the studied populations. The translocation factor coefficient for Fe in the shoot wood of willows from LYR 8 was also higher than 1.

In bark, absolute concentrations of Cd, Fe, Mg, Mn, and Zn were markedly higher than in wood, especially for Fe. Statistically, the highest amount of Fe was found in the shoot bark of the LYR 4 population, while the lowest amount was found in the root bark of the LYR 3 and LYR 8 populations. For Cd and Cu, changes in the content of elements in the bark of shoots and roots corresponded to the relationships observed in wood. For Mg, no significant differences in accumulation were measured between sites or plant organs. The highest Mn accumulation was recorded in the root bark of the LYR 4 population, while the lowest values were measured in the bark of the LYR 8 population. The highest copper concentrations were detected in the root bark of LYR 4, similar to the accumulation of this metal in wood. We demonstrated increased accumulation of heavy metals (Cd, Zn), but also Mn, in the tissues of *S. polaris* growing at higher elevations compared to valley sites. We measured significantly higher concentrations of all investigated metals in *S. polaris* bark than in wood (Fig. 3). At low elevation, we detected maximum Cd content in *S. polaris* shoot at 4.7 ppm, whereas at an altitude of 400 m above valley bottom this value was as high as 13 ppm (Fig. 3). The same was the case for Zn, when in the higher-located populations the metal accumulation reached a record 1200 ppm, while in the valley the maximum values did not exceed 600 ppm (Fig. 3).

The question arises as to whether pollution can affect the width of annual growth rings of *S. polaris*? As a result of dendrochronological research, two chronologies of annual growth widths were compiled, covering the years 1988–2022 for LYR 3 and LYR 4 sites and 1992–2022 for LYR 8 site. The width of annual increments in high and low elevation sites is characterised by very high variability, which is typical for *S. polaris* (Fig. 4). Although certain sections of dendrochronological scales show similarities in their course, like the rain-on-snow event in 2014, there is nevertheless a noticeable heterogeneity in their patterns (Fig. 4). Narrower rings were found at higher altitudes (mean growth ring width: 64 μm) than at lower ones (mean growth ring width: 102.4 μm) (Fig. 4). The most important factor influencing this trend appears to be altitude and harsher growing conditions. Conversely, although the growing season is longer at lower altitudes, drought stress occurs in the second half of the season. Therefore, wider growth rings may primarily be the result of a higher content of exchangeable cations and elements available to plants in the topsoil. Taking this into account, it can be assumed that in higher locations, in addition to climatic conditions, high concentrations of pollutants will also contribute to a reduction in the width of the growth rings.

Soil characteristics

The studied topsoils were characterized by acidic (sites: LYR 3 and LYR 4) and slightly acidic reaction (site LYR 8), due to lack of carbonates in the parent material. The topsoils occurring in mountain area showed lower content of SOC and TN as well as C/N ratio in comparison with the topsoil from the Longyeardalen valley (Table 1). Chemical composition of all the topsoils was similar (Table 1); however, topsoils occurring in the mountains (sites: LYR 3 and LYR 4) contained higher amount of SiO_2, and slightly lower amount of Al_2O_3, Fe_2O_3, MgO, CaO, Na_2O, and K_2O than topsoil from the Longyeardalen valley (site LYR 8). The chemical composition of the topsoils is associated with highly siliceous parent material (Table 1), *i.e.*, residues of sandstones and siltstones, which prevail in this area (Dallmann *et al.* 2001; Szymański *et al.* 2019). The topsoil from the Longyeardalen valley showed clearly higher concentration of Ca^{2+} and slightly higher concentration of Mg^{2+} as well as lower concentration of H^+ and Al^{3+} than the topsoils from mountains and this is main reason of slightly higher pH of the topsoil from the valley. In addition, concentrations of plant available potassium and magnesium were higher in the topsoil from the valley than from the mountains (Table 1). All the topsoils showed loamy texture, *i.e.*, loam or sandy loam (Table 1), because weathering of clastic rocks such as sandstone, siltstone and shale leads to formation of residues and deposits showing loamy texture. However, topsoils from mountains were characterized by higher content of sand fraction and lower content of silt fraction than topsoil from the valley, which is most likely related to local heterogeneity of residues as well as wind activity.

Principal component analysis

The selected variables explained nearly 88% of the total variance, which supports the identification of significant regularities in this analysis (Fig. 5). Principal component analysis confirmed the importance of soil pH and SOC in differentiating populations and in metal accumulation. *Salix polaris* populations clustered along an elevation gradient, as did heavy metal contamination, supporting the fog deposition hypothesis. The analysis also confirmed a negative correlation between annual wood growth and elevation above the valley floor. The analysis also showed that Zn content in *S. polaris* bark was nonspecific, unlike the accumulation of this metal in wood.

Discussion

Metal content in the plants

Heavy metals are important environmental pollutants that can affect Svalbard's ecosystems, as well as those across the entire Arctic, both directly and indirectly. In addition to the primary sources of pollution, such as long-range and local transport pathways, pollutants present in the terrestrial environment are also released from secondary sources, such as riverine runoff (Rudnicka-Kępa and Zaborska 2021). Although the overall influx and transport of pollutants is relatively well understood (Zaborska *et al.* 2017), little is known about their spatial distribution in relation to the topography, altitude, and their concentration in the different anatomical parts of Arctic woody plants. The metal concentrations we measured were within the physiological ranges already published for *S. polaris* (Wojtuń *et al.* 2019) and *S. arctica* (Ermakov *et al.* 2015). Significantly higher concentrations of metals in willow bark than in wood detected in all sites confirms the results obtained for other willow species (Zárubová *et al.* 2015) and for birch (Sitko *et al.* 2021). Wojtuń *et al.* (2019) measured the maximum Cd content in *S. polaris* shoots in Longyearbyen at 5.0 ppm, while our maximum for this population was 4.7 ppm. At the same time, populations located 400 m above the valley bottom reached maximum Cd accumulation of 13 ppm. The same was the case for Zn, when in the higher-located populations the metal accumulation reached a record 1200 ppm, while in the valley the maximum values were half as high, and in previous research with the maximum at 433 ppm (Wojtuń *et al.* 2019). On the one hand, our results are strongly related to the studies of our predecessors; on the other hand, they shed new light on the increase in metal accumulation in plant tissues, including toxic trace metals such as Cd and Zn, at higher-lying sites.

The annual growth rings of *S. polaris* are characterised by very high variability, which is typical for Arctic shrubs (Owczarek and Opała 2016; Le Moullec *et al*. 2019; Opała-Owczarek *et al*. 2019; Owczarek *et al*. 2021; Phulara *et al*. 2025). Wider ring widths were observed at lower altitudes. Given the adverse effects of drought stress at lower altitudes during the second half of the growing season, these higher values should be attributed to nutrient supply and better physicochemical soil conditions, *e.g.*, high concentration Ca^{2+} and Mg^{2+} in comparison with sites located at higher altitudes (Phulara *et al*. 2025). Higher contents of soil organic carbon, total nitrogen and the C/N ratio, compared with sites located on the plateau, indicate better soil conditions that may offset the negative impact of drought stress at lower elevations. These relationships between the physicochemical properties of the soil and the development of vegetation cover in central Spitsbergen have previously been described by Szymański *et al.* (2019) and Bartos *et al.* (2023, 2024). At higher altitudes in central Spitsbergen, no negative impact of drought stress on annual ring width was observed, as described in detail by Phulara *et al*. (2025). Consequently, the significantly narrower ring widths at higher altitudes may be due not only to the slightly poorer physicochemical properties of the topsoil, but also to the impact of environmental pollution. To date, no research has been conducted on the impact of pollution on the reduction of annual growth in Arctic shrubs. Nevertheless, this concern has been thoroughly researched, for example in polluted areas of the Russian subarctic (Nöjd and Reams 1996; Kirdyanov *et al.* 2014; Kharuk *et al.* 2023) and in the mountains of Central Europe (Opala-Owczarek *et al.* 2018; Myśkow *et al.* 2019). In the case of long-term increment series obtained from trees growing in areas subject to strong pollution pressure, reductions in increment width for the period of highest contamination and a change or weakening of the dendroclimatic signal are characteristic. However, the length of the *S. polaris* increment chronology is insufficient for a comparative analysis of the polluted and unpolluted sub-periods. Further research in dendroecology and dendrochemistry of Arctic tundra plants will require the inclusion of additional reference sites or the discovery of older specimens dating from times before the increase in pollution emissions to fully assess the impact of pollution on the dendrochronological record, as well as ultra-high-resolution analyses of isotopic and elemental composition in individual annual growth rings. Ring-resolved micro-analyses (*e.g.*, LA-ICP-MS, µXRF) should be used to build year-by-year metal series and directly test the fog-interception mechanism. Overall, bark captures recent inputs, xylem integrates longer-term exposure, and elevation/site context modulates both, supporting *S. polaris* as a practical indicator system for distinguishing between near-term deposition and longer-term uptake, and for tracking metal contamination in a rapidly changing High-Arctic environment. Progress in specific disciplines, analytical advances, and large-scale pan-Arctic sampling campaigns aiming at complex analysis of environmental effects on shrubs growth, will increase the research potential of shrub and dwarf shrubs growth-rings.

Effect of fog pollution

Our research indicates that the content of pollutants in plants growing at an altitude of > 400 m a.s.l. is almost 2–3 times higher than in the valleys. This may be related to the Arctic Atmospheric Boundary Layer (ABL) and the so-called "pollutant fog deposition". The prevalent presence of fog/cloud at a given altitude may be crucial in the accumulation of pollutants and affect the width of annual increments (Myśkow *et al.* 2019). Pollutant concentrations in clouds or fog are usually several times higher than in atmospheric precipitation (Błaś *et al.* 2012). Research conducted in the Sudetes Mountains, near the upper forest limit, indicates that total pollutant deposition consisted of 35–50% direct deposition from fog and clouds. In nearby lowland areas, by contrast, this proportion was just 5% (Błaś *et al.* 2008).

Research on long-range transport (LRT) of atmospheric pollutants shows that their transport and deposition depend on mesoscale atmospheric circulation mechanisms, the characteristics of the atmospheric boundary layer and climate, and orography (Dore *et al.* 1999; Błaś *et al.* 2012). These factors lead to significant vertical variations in the deposition of pollutants, particularly at the interface between the vertical thermal inversion and ABL. This is particularly evident in the base zone of lower-level clouds and orographic clouds and fog. Changes in the height of the ABL and in the air temperature in the vertical profile mark the boundary between the dynamics of processes involved in cloud development and the surface radiation budget. As a result, the structure of the ABL modifies precipitation chemistry and the dynamics of other meteorological processes, *e.g.*, water income from the atmosphere. The Arctic is characterised by stable ABL (Kral *et al.* 2021). Consequently, there is no vertical cloud development, and stratus and stratocumulus clouds prevail. These clouds often have a base at an altitude of 400–600 m a.s.l., *i.e.*, at the boundary of the mixing layer (Fig. 6) (Kilpeläinen *et al.* 2012; Maturilli and Ebell 2018; Maturilli 2022; Suomi *et al.* 2025). This relatively low ABL elevation is observed in summer, while in spring the ABL can reach up to 1000 m (Cheng-Ying *et al.* 2011).

In the process of cloud formation, natural and anthropogenic atmospheric pollutants act as condensation nuclei, while the clouds themselves trap the dry fraction of transported pollutants. It is in the zone where lower-level clouds form and occur, at an altitude of 400–600 m a.s.l., that pollutants are captured and concentrated (Fig. 6). This mechanism, originally proposed by Bergeron (1965) is known as the ”seeder – feeder effect". This mechanism typically causes an increase in precipitation relative to the lower elevation (Dore *et al.* 1999; Błaś *et al.* 2012). Because of this mechanism orographic cloud droplets are scavenged by upper-level precipitation leading to a significant increase of both precipitation and pollutant deposition. Heavily polluted cloud and fog droplets are deposited on the ground as precipitation or atmospheric deposits. These droplets can make a significant contribution to the water balance, and by supplying plants with water they can introduce pollutants such as heavy metals or sulphur compounds into them. The deposition of fog pollutants can directly damage tissue, causing erosion of waxy coatings and lesions. This can lead to leaf yellowing and, consequently, reduced growth (Myśkow *et al.* 2019).

There are some uncertainties associated with the lack of data on fog chemistry or the influence of microtopography, which can modulate bioavailability. However, these doubts can be reduced by pairing tissues with co-located soil/snow/fog chemistry and meteorology, standardizing shrub size/age, and periodically resampling marked shrubs.

Conclusions

For the first time in the Arctic, our research indicated increased metal accumulation in *Salix polaris* tissues at higher elevations, which is consistent with enhanced fog and low-cloud deposition. This phenomenon can be linked to the Arctic Atmospheric Boundary Layer and the so-called “pollutant fog deposition”. It should be noted that our findings are proposed based on consistency between the spatial pattern of metal accumulation and topographical and meteorological conditions rather than direct confirmation by measurements of fog chemistry, precipitation, aerosols or atmospheric deposition. Previous studies on metal accumulation in plants have focused on the impact of local pollution sources without analysing the vertical distribution of contamination. Across the gradient, metal concentrations in *S. polaris* were higher at high elevation and lower at the valley floor, most clearly in bark. Therefore, this part of the plant, as a bioindicator of pollution, should be taken into account first and foremost when assessing the condition of the natural environment. On average, metal content in bark and wood in shoots and roots at 420–460 m a.s.l. were 2–3 times higher than at the valley bottom. The pattern is consistent with enhanced delivery via polluted fog/low-cloud interception at higher elevations, superimposed on local dust resuspension. These significant levels of metal contamination may affect the growth of polar willow and reduce the width of its annual growth rings, although this is obviously exacerbated by harsh climatic conditions. Further detailed research is needed to clarify these uncertainties, covering not only parts of the plant, but the annual growth rings themselves in particular. Based on the discovered relationships, it is proposed that monitoring of heavy metal concentrations in the Arctic environment should be expanded to include analysis of the height of the Arctic Boundary Layer, in order to determine the potential for increased pollution levels at higher altitudes.

Acknowledgements

The results presented in this paper were obtained within the project No. 2021/41/B/ST10/03381"*Spatio-temporal patterns in Arctic tundra greening and browning—identification of key environmental factors (TURNING)*" financed by the Polish National Science Centre. The study was carried out with a permit from the Governor of Svalbard (RIS-ID 12030). Our thanks are due to Katarzyna Jankowska and the anonymous reviewer for their constructive comments that greatly improved the manuscript.

References

Afflerbach J.C., Yocum D. and Halpern B.S. 2017. Cumulative human impacts in the Bering Strait Region. *Ecosystem Health and Sustainability* 3: 1379888.

AMAP 2015. *Radioactivity in the Arctic*. Arctic Monitoring and Assessment Programme (AMAP), Oslo, Norway

AMAP 2021. Assessment 2020: *POPs and chemicals of emerging arctic concern: influence of Climate Change*. Arctic Monitoring and Assessment Programme (AMAP), Tromsø, Norway.

Anisimov O.A., Vaughan D.G., Callaghan T.V., C. Furgal C., Marchant H., Prowse T.D., Vilhjálmsson H. and Walsh J.E. 2007. Polar regions (Arctic and Antarctic). *In:* Parry M.L., Canziani O.F., Palutikof J.P., van der Linden P.J. and Hanson C.E. (eds.) *Climate Change 2007: Impacts,* *Adaptation and Vulnerability. Contribution of Working Group II to the Fourth As-sessment Report of the Intergovernmental Panel on Climate Change*. Cambridge University Press, Cambridge.

Askaer L., Schmidt L.B., Elberling B., Asmund G. and Jónsdóttir I.S. 2008. Environmental impact on an Arctic soil–plant system resulting from metals released from coal mine waste in Svalbard (78 N). *Water, air, and soil pollution* 195: 99–114.

Bard S.M. 1999. Global transport of anthropogenic contaminants and the consequences for the Arctic marine ecosystem. *Marine Pollution Bulletin* 38: 356–379.

Bargagli R. 2016. Moss and lichen biomonitoring of atmospheric mercury: A review. *Science of the Total Environment* 572: 216–231, doi: 10.1016/j.scitotenv.2016.07.202.

Bartos A., Szymański W. and Gus-Stolarczyk M. 2023. Morphology and properties of permafrost-affected soils under different tundra vegetation in central Spitsbergen. *Polish Polar Research* 44: 1–20, doi: 10.24425/ppr.2022.143317.

Bartos A., Stolarczyk M. and Szymański W. 2024. Content and quality of soil organic matter in topsoils under different tundra vegetation in central Spitsbergen (High Arctic). *Geoderma Regional* 39: e00891.

Bergeron T. 1965. On the low-level redistribution of atmospheric water caused by orography. *Proceedings of the International Conference on Cloud Physics*, Tokyo and Sapporo, Japan, 24 May–1 June 1965: 96–100.

Birks H.J.B., Jones V.J. and Rose N.L. 2004. Recent environmental change and atmospheric contamination on Svalbard as recorded in lake sediments–an introduction. *Journal of Paleolimnology* 31: 403–410.

Błaś M., Sobik M. and Twarowski R. 2008. Changes of cloud water chemical composition in the Western Sudety Mountains, Poland. *Atmospheric Research* 87: 224–231.

Błaś M., Sobik M., Polkowska Ż., Cichała-Kamrowska K. and Namieśnik J. 2012. Water and chemical properties of hydrometeors over Central European mountains. *Pure and Applied Geophysics* 169: 1067–1081.

Braun-Blanquet J. 1964. *Die grundlegenden Vegetationseinheiten, ihr Gefüge und ihre Erfassung*. Springer, Vienna: 17–205, doi: 10.1007/978-3-7091-8110-2_3.

Buchwal A., Rachlewicz G., Fonti P., Cherubini P. and Gartner H. 2013. Temperature modulates intra-plant growth of *Salix polaris* from a high Arctic site (Svalbard). *Polar Biology* 36: 1305–1318, doi: 10.1007/s00300-013-1349-x.

Cecinato A., Mabilia R. and Marino F. 2000. Relevant organic components in ambient particulate matter collected at Svalbard Islands (Norway). *Atmospheric Environment* 34: 5061–5066.

Cheng-Ying D., Zhi-Qiu G., Qing W. and Gang C. 2011. Analysis of atmospheric boundary layer height characteristics over the Arctic Ocean using the aircraft and GPS soundings. *Atmospheric and Oceanic Science Letters* 4: 124–130.

Chiarantini L., Rimondi V., Benvenuti M., Beutel M.W., Costagliola P., Gonnelli C., Lattanzi P. and Paolieri M. 2016. Black pine (*Pinus nigra*) barks as biomonitors of airborne mercury pollution. *Science of the Total Environment* 569: 105–113, doi: 10.1002/ppp.523.

Cocozza C., Ravera S., Cherubini P., Lombardi F., Marchetti M. and Tognetti R. 2016. Integrated biomonitoring of airborne pollutants over space and time using tree rings, bark, leaves and epiphytic lichens. *Urban Forestry & Urban Greening* 17: 177–191, doi: 10.1016/j.ufug.2016.04.008.

Cook E. and Holmes R. 1996. Guide for computer program ARSTAN. *In*: Grissino-Mayer H.D., Holmes R.L. and Fritts H.C. (eds.) *The international tree-ring data bank program library version 2.0 user's manual. 2*, University of Arizona, Tucson, AZ: 75–87.

Dallmann W., Kjærnet T. and Nøttvedt A. 2001. *Geomorphological and Quaternary Map of Svalbard. 1: 100,000, Sheet C9G Adventdalen, Temakart No. 31/32*. Norwegian Polar Institute, Tromsø.

Dore A., Sobik M. and Migala K. 1999. Patterns of precipitation and pollutant deposition in the western Sudete mountains, Poland. *Atmospheric Environment* 33: 3301–3312.

Drbal K., Elster J. and Komarek J. 1992. Heavy metals in water, ice and biological material from Spitsbergen, Svalbard. *Polar Research* 11: 99–101.

Dziurowicz P., Fałowska P., Waszkiewicz K., Kamiński A., Nicia P., Zadrożny P., Bejger R., Owczarek P., Opała-Owczarek M., Szymański W., Korabiewski B. and Węgrzyn M.H. 2025. Metal bioaccumulation and physiological responses of Arctic lichens under climate change and pollution. *Ecological Indicators* 178: 113959, doi: 10.1016/j.ecolind.2025.113959.

Elvebakk A. 1994. A survey of plant associations and alliances from Svalbard. *Journal of Vegetation Science* 5: 791–802.

Elvebakk A. 1997. Tundra diversity and ecological characteristics of Svalbard. *In*: Wielgolaski F.E. (ed.) *Ecosystems of the world 3. Polar and Alpine Tundra*. Elsevier, Amsterdam-Tokyo: 347–360.

Elvebakk A. 2005. A vegetation map of Svalbard on the scale 1: 3.5 mill. *Phytocoenologia* 35: 951–967.

Elvebakk A. and Prestrud P. 1996. *A catalogue of Svalbard plants, fungi, algae and cyanobacteria*. Norsk Polarinstitutt, Oslo.

Ermakov V.V., Petrunina N.S., Tyutikov S.F., Danilova V.N., Khushvakhtova S.D., Degtyarev A.P. and Krechetova E.V. 2015. Concentrating metals by plants of the genus Salix and their importance for identification of Cd anomalies. *Geochemistry International* 53: 951–963, doi: 10.1134/S0016702915110026.

Gallet J., Björkman M., Borstad C., Hodson A., Jacobi H., Larose C., Luks B., Spolaor A., Urazgildeeva A. and Zdanowicz C. 2019. Snow research in Svalbard: current status and knowledge gaps. State of Environmental Science in Svalbard (SESS) report 2018.

Gärtner H. and Schweingruber F.H. 2013. *Microscopic preparation techniques for plant stem analysis*. Kessel Publishing House, Remagen, Germany.

Gärtner H., Lucchinetti S. and Schweingruber F.H. 2014. New perspectives for wood anatomical analysis in dendrosciences: the GSL1-microtome. *Dendrochronologia* 32: 47–51.

Gee G.W. and Bauder J.W. 1986. Particle-size analysis. *In:* Klute A. (ed.) *Methods of soil analysis: Part 1 Physical and mineralogical methods*. American Society of Agronomy, Inc., and Soil Science Society of America, Inc., Madison: 383–411.

Grissino-Mayer H.D. 2001. Evaluating crossdating accuracy: a manual and tutorial for the computer program COFECHA. *Tree-Ring Research* 57: 205–221.

Grodzińska K. and Godzik B. 1991. Heavy metals and sulphur in mosses from southern Spitsbergen. *Polar Research* 9: 133–140.

Gworek B., Dmuchowski W. and Baczewska-Dąbrowska A.H. 2020. Mercury in the terrestrial environment: a review. *Environmental Sciences Europe* 32: 128, doi: 10.1186/s12302-020-00401-x.

Headley A.D. 1996. Heavy metal concentrations in peat profiles from the high Arctic. *Science of the Total Environment* 177: 105–111.

Hjelle A. 1993. *Geology of Svalbard*. Polarhandbok 7. Norsk Polarinstitutt, Oslo

Huntington H.P., Olsen J., Zdor E., Zagorskiy A., Shin H.C., Romanenko O., Kaltenborn B., Dawson J., Davies J. and Abou-Abbsi E. 2023. Effects of Arctic commercial shipping on environments and communities: context, governance, priorities. *Transportation Research Part D: Transport and Environment* 118: 103731, doi: 10.1016/j.trd.2023.103731.

Ismael M.A., Elyamine A.M., Moussa M.G., Cai M., Zhao X. and Hu C. 2019. Cadmium in plants: uptake, toxicity, and its interactions with selenium fertilizers. *Metallomics* 11: 255–277, doi: 10.1039/c8mt00247a.

Jóźwik Z. 2000. Heavy metals in tundra plants of the Bellsund in West Spitsbergen, investigated in the years 1987–1995. *Polish Polar Research* 21: 401–409.

Kharuk V.I., Petrov I.y.A., Im S.T., Golyukov A.S., Dvinskaya M.L. and Shushpanov A.S. 2023. Pollution and climatic influence on trees in the Siberian Arctic wetlands. *Water* 15: 215, doi: 10.3390/w15020215.

Kilpeläinen T., Vihma T., Manninen M., Sjöblom A., Jakobson E., Palo T. and Maturilli M. 2012. Modelling the vertical structure of the atmospheric boundary layer over Arctic fjords in Svalbard. *Quarterly Journal of the Royal Meteorological Society* 138: 1867–1883, doi: 10.1002/qj.1914.

Kirdyanov A.V., Myglan V.S., Pimenov A.V., Knorre A.A., Ekart A.K. and Vaganov E.A. 2014. Die-off dynamics of Siberian larch under the impact of pollutants emitted by Norilsk enterprises. *Contemporary Problems of Ecology* 7: 679–684, doi: 10.1134/S1995425514060055.

Kolishchuk V. 1990. Dendroclimatological study of prostrate woody plants. *In*: Cook E.R. and Kairiukstis L.A. (eds): *Methods of Dendrochronology: Applications in the Environmental Sciences*. London, Springer Netherlands: 51–55.

Kral S.T., Reuder J., Vihma T., Suomi I., Haualand K.F., Urbancic G.H., Greene B.R., Steeneveld G.-J., Lorenz T. and Maronga B. 2021. The innovative strategies for observations in the Arctic Atmospheric Boundary Layer Project (ISOBAR): Unique finescale observations under stable and very stable conditions. *Bulletin of the American Meteorological Society* 102: E218–E243.

Kuo S. 1996. Phosphorus. *In*: Sparks D.L. (ed.) *Methods of Soil Analysis: Part 3,* SSSA Book Series No. 5, SSSA and ASA, Madison: 869–919.

Law K.S. and Stohl A. 2007. Arctic air pollution: Origins and impacts. *Science* 315: 1537–1540.

Le Moullec M., Buchwal A., van der Wal R., Sandal L. and Hansen B.B. 2019. Annual ring growth of a widespread high arctic shrub reflects past fluctuations in community-level plant biomass. *Journal of Ecology* 107: 436–451, doi: 10.1111/1365-2745.13036.

Łokas E., Zaborska A., Sobota I., Gaca P., Milton J.A., Kocurek P. and Cwanek A. 2019. Airborne radionuclides and heavy metals in high Arctic terrestrial environment as the indicators of sources and transfers of contamination. *The Cryosphere* 13: 2075–2086, doi: 10.5194/tc-13-2075-2019.

Małecki J. 2016. Accelerating retreat and high-elevation thinning of glaciers in central Spitsbergen. *The Cryosphere* 10: 1317–1329, doi: 10.5194/tc-10-1317-2016.

Martin A.C., Jeffers E.S., Petrokofsky G., Myers-Smith I. and Macias-Fauria M. 2017. Shrub growth and expansion in the Arctic tundra: an assessment of controlling factors using an evidence-based approach. *Environmental Research Letters* 12: 085007, doi: 10.1088/1748-9326/aa7989.

Martin J.A.R., Gutiérrez C., Torrijos M. and Nanos N. 2018. Wood and bark of Pinus halepensis as archives of heavy metal pollution in the Mediterranean Region. *Environmental Pollution* 239: 438–447.

Maturilli M. 2022. Ceilometer cloud base height from station Ny-Ålesund (2017-08 et seq). PANGAEA, doi: 10.1594/PANGAEA.942331.

Maturilli M. and Ebell K. 2018. Twenty-five years of cloud base height measurements by ceilometer in Ny-Ålesund, Svalbard. *Earth System Science Data* 10: 1451–1456, doi: 10.5194/essd-10-1451-2018.

Myers-Smith I.H., Hallinger M., Blok D., Sass-Klaassen U., Rayback S.A., Weijers S., Trant A.J., Tape K.D., Naito A.T., Wipf S., Rixen C., Dawes M.A., Wheeler J.A., Buchwal A., Baittinger C., Macias-Fauria M., Forbes B.C., Levesque E., Boulanger-Lapointe N., Beil I., Ravolainen V. and Wilmking M. 2015. Methods for measuring arctic and alpine shrub growth: A review. *Earth-Science Reviews* 140: 1–13, doi: 10.1016/j.earscirev.2014.10.004.

Myers-Smith I.H., Kerby J.T., Phoenix G.K., Bjerke J.W., Epstein H.E., Assmann J.J., John C., Andreu-Hayles L., Angers-Blondin S., Beck P.S.A., Berner L.T., Bhatt U.S., Bjorkman A.D., Blok D., Bryn A., Christiansen C.T., Cornelissen J.H.C., Cunliffe A.M., Elmendorf S.C., Forbes B.C., Goetz S.J., Hollister R.D., de Jong R., Loranty M.M., Macias-Fauria M., Maseyk K., Normand S., Olofsson J., Parker T.C., Parmentier F.J.W., Post E., Schaepman-Strub G., Stordal F., Sullivan P.F., Thomas H.J.D., Tommervik H., Treharne R., Tweedie C.E., Walker D.A., Wilmking M. and Wipf S. 2020. Complexity revealed in the greening of the Arctic. *Nature Climate Change* 10: 106–117, doi: 10.1038/s41558-019-0688-1.

Myśkow E., Błaś M., Sobik M., Godek M. and Owczarek P. 2019. The effect of pollutant fog deposition on the wood anatomy of subalpine Norway spruce. *European Journal of Forest Research* 138: 187–201, doi: 10.1007/s10342-018-01160-4.

Nawrot A.P., Migała K., Luks B., Pakszys P. and Głowacki P. 2016. Chemistry of snow cover and acidic snowfall during a season with a high level of air pollution on the Hans Glacier, Spitsbergen. *Polar Science* 10: 249–261.

Nöjd P. and Reams G.A. 1996. Growth variation of Scots pine across a pollution gradient on the Kola Peninsula, Russia. *Environmental Pollution* 93: 313–325, doi: 10.1016/S0269-7491(96)00049-8.

Opała-Owczarek M., Piroznikow E., Owczarek P., Szymanski W., Luks B., Kepski D., Szymanowski M., Wojtun B. and Migala K. 2018. The influence of abiotic factors on the growth of two vascular plant species (*Saxifraga oppositifolia* and *Salix polaris*) in the High Arctic. *Catena* 163: 219–232, doi: 10.1016/j.catena.2017.12.018.

Opała-Owczarek M., Błaś M., Owczarek P., Sobik M. and Godek M. 2019. A dendroclimatological study of east-and west-facing slopes in mountainous areas subjected to strong air pollution (the Sudetes, Central Europe). *Physical Geography* 40: 186–208.

Owczarek P. and Opała M. 2016. Dendrochronology and extreme pointer years in the tree-ring record (AD 1951–2011) of polar willow from southwestern Spitsbergen (Svalbard, Norway). *Geochronometria* 43: 84–95, doi: 10.1515/geochr-2015-0035.

Owczarek P., Latocha A., Wistuba M. and Malik I. 2013. Reconstruction of modern debris flow activity in the arctic environment with the use of dwarf shrubs (south-western Spitsbergen) - a new dendrochronological approach. *Zeitschrift Fur Geomorphologie* 57: 75–95, doi: 10.1127/0372-8854/2013/S-00145.

Owczarek P., Nawrot A., Migała K., Malik I. and Korabiewski, B. 2014. Flood-plain responses to contemporary climate change, Svalbard. *Boreas* 43: 384–402, doi: 10.1111/bor.12061.

Owczarek P., Opala-Owczarek M. and Migala K. 2021. Post-1980s shift in the sensitivity of tundra vegetation to climate revealed by the first dendrochronological record from Bear Island (Bjørnøya), western Barents Sea. *Environmental Research Letters* 16: 014031, doi: 10.1088/1748-9326/abd063.

Phulara M., Opała-Owczarek M., Szymański W., Ślopek J., Węgrzyn M., Łupikasza E., Korabiewski B. and Owczarek P. 2025. Multiple factors controlling polar willow growth in the high Arctic (Svalbard): Implications for future prediction of tundra productivity. *Global Ecology and Conservation* 62: e03801, doi: 10.1016/j.gecco.2025.e03801.

Rinn F. 2003. *TSAP-Win Professional–Zeitreihenanalyse und Präsentation für Dendrochronologie und verwandte Anwendungen.* Rinntech, Heidelberg, Germany.

Rodríguez Martín J.A., Nanos N., Grigoratos T., Carbonell G. and Samara C. 2014. Local deposition of mercury in topsoils around coal-fired power plants: is it always true? *Environmental Science and Pollution Research* 21: 10205–10214.

Rønning O. 1996. *The Flora of Svalbard*. Norsk Polarinstitutt, Oslo.

Rudnicka-Kępa P. and Zaborska A. 2021. Sources, fate and distribution of inorganic contaminants in the Svalbard area, representative of a typical Arctic critical environment–a review. *Environmental Monitoring and Assessment* 193: 724, doi: 10.1007/s10661-021-09305-6.

Saarela K.E., Harju L., Rajander J., Lill J.O., Heselius S.J., Lindroos A. and Mattsson K. 2005. Elemental analyses of pine bark and wood in an environmental study. *Science of the Total Environment* 343: 231–241, doi: 10.1016/j.scitotenv.2004.09.043.

Sawidis T., Breuste J., Mitrovic M., Pavlovic P. and Tsigaridas K. 2011. Trees as bioindicator of heavy metal pollution in three European cities. *Environmental Pollution* 159: 3560–3570, doi: 10.1016/j.envpol.2011.08.008.

Schachtschabel P. 1954. Plant-available magnesium in soil and its determination. *Zeitschrift für Pflanzenernährung, Düngung und Bodenkunde* 67: 9–23.

Schaefer K., Elshorbany Y., Jafarov E., Schuster P.F., Striegl R.G., Wickland K.P. and Sunderland E.M. 2020. Potential impacts of mercury released from thawing permafrost. *Nature Communications* 11: 4650, doi: 10.1038/s41467-020-18398-5.

Simões J.C. and Zagorodnov V.S. 2001. The record of anthropogenic pollution in snow and ice in Svalbard, Norway. *Atmospheric Environment* 35: 403–413.

Sitko K., Opała-Owczarek M., Jemioła G., Gieroń Ż., Szopiński M., Owczarek P., Rudnicka M. and Małkowski E. 2021. Effect of drought and heavy metal contamination on growth and photosynthesis of silver birch trees growing on post-industrial heaps. *Cells* 11: 53, doi: 10.3390/cells11010053.

Stock M., Ritter C., Aaltonen V., Aas W., Handorff D., Herber A., Treffeisen R. and Dethloff K. 2014. Where does the optically detectable aerosol in the European Arctic come from? *Tellus B: Chemical and Physical Meteorology* 66: 21450, doi:10.3402/tellusb.v66.21450.

Summer M. 1992. Determination of exchangeable acidity and exchangeable Al using 1 N KCl. *In:* Donohue S.J. (ed.) *Reference soil and media diagnostic procedures for the Southern Region of the United States*. Southern Cooperative Series Bulletin Number 374, Virginia Agricultural Experiment Station, VPI & SU, Blacksburg: 41–42.

Sumner M.E. and Miller W.P. 1996. Cation exchange capacity and exchange coefficients. *In:* Sparks D.L., Page A.L., Helmke P.A., Loeppert R.H., Soltanpour P.N., Tabatabai M.A., Johnston C.T. and Sumner M.E. (eds.) *Methods of soil analysis: Part 3 Chemical methods.* American Society of Agronomy, Crop Science Society of America, and Soil Science Society of America: 1201–1229, doi: 10.2136/sssabookser5.3.c40.

Suomi J., Hyyrynen M., Käyhkö J., Käyhkö J. and Juhola S. 2025. Economic viability of urban greening as a climate change adaptation measure in cool-climate cities. *Regional Environmental Change* 25: 95.

Szymański W., Siwek J., Skiba M., Wojtuń B., Samecka-Cymerman A., Pech P., Polechońska L. and Smyrak-Sikora A. 2019. Properties and mineralogy of topsoil in the town of Longyearbyen (Spitsbergen, Norway). *Polar Record* 55: 102–114, doi: 10.1017/S0032247419000251.

Szymański W., Drewnik M., Stolarczyk M., Musielok Ł., Gus-Stolarczyk M. and Skiba M. 2022a. Occurrence and stability of organic intercalation in clay minerals from permafrost-affected soils in the High Arctic–A case study from Spitsbergen (Svalbard). *Geoderma* 408: 115591, doi: 10.1016/j.geoderma.2021.115591.

Szymański W., Jagi K., Drewnik M., Musielok Ł., Stolarczyk M., Gus-Stolarczyk M. and Sikora S. 2022b. Impact of tundra vegetation type on topsoil temperature in central Spitsbergen (Svalbard, High Arctic). *Geoderma* 428: 116196, doi: 10.1016/j.geoderma.2022.116196.

Thomas G.W. 1996. Soil pH and soil acidity. *In:* Sparks D.L., Page A.L., Helmke P.A., Loeppert R.H., Soltanpour P.N., Tabatabai M.A., Johnston C.T. and Sumner M.E. (eds.) *Methods of soil analysis: Part 3 Chemical methods.* American Society of Agronomy, Crop Science Society of America, and Soil Science Society of America: 475–490.

Walker D.A., Raynolds M.K., Daniels F.J.A., Einarsson E., Elvebakk A., Gould W.A., Katenin A.E., Kholod S.S., Markon C.J., Melnikov E.S., Moskalenko N.G., Talbot S.S., Yurtsev B.A. and Team C. 2005. The Circumpolar Arctic vegetation map. *Journal of Vegetation Science* 16: 267–282, doi: 10.1658/1100-9233(2005)016.

Węgrzyn M. and Wietrzyk P. 2015. Phytosociology of snowbed and exposed ridge vegetation of Svalbard. *Polar Biology* 38: 1905–1917, doi: 10.1007/s00300-015-1751-7.

Weinbruch S., Drotikova T., Benker N. and Kallenborn R. 2015. Particulate and gaseous emissions of power generation at Svalbard (AtmoPart). *ATMOPART Final report 2015,* Svalbard Environmental Protection Fund, Longyearbyen, Norway.

Wojtuń B., Samecka-Cymerman A., Kolon K. and Kempers A.J. 2018. Metals in *Racomitrium lanuginosum* from Arctic (SW Spitsbergen, Svalbard archipelago) and alpine (Karkonosze, SW Poland) tundra. *Environmental Science and Pollution Research* 25: 12444–12450, doi: 10.1007/s11356-018-1508-2.

Wojtuń B., Polechońska L., Pech P., Mielcarska K., Samecka-Cymerman A., Szymański W., Kolon M., Kopeć M., Stadnik K. and Kempers A.J. 2019. *Sanionia uncinata* and *Salix polaris* as bioindicators of trace element pollution in the High Arctic: A case study at Longyearbyen, Spitsbergen, Norway. *Polar Biology* 42: 1287–1297, doi: 10.1007/s00300-019-02517-0.

Zaborska, A., Beszczyńska-Möller, A., and Włodarska-Kowalczuk, M. 2017. History of heavy metal accumulation in the Svalbard area: Distribution, origin and transport pathways. *Environmental Pollution* 231: 437–450, doi: 10.1016/j.envpol.2017.08.042.

Zárubová P., Hejcman M., Vondráčková S., Mrnka L., Száková J. and Tlustoš P. 2015. Distribution of P, K, Ca, Mg, Cd, Cu, Fe, Mn, Pb and Zn in wood and bark age classes of willows and poplars used for phytoextraction on soils contaminated by risk elements. *Environmental Science and Pollution Research* 22: 18801–18813, doi: 10.1007/s11356-015-5043-0.

Zhou J., Wen Y., Marshall M.R., Zhao J., Gui H., Yang Y., Zeng Z., Jones D.L. and Zang H. 2021. Microplastics as an emerging threat to plant and soil health in agroecosystems. *Science of the Total Environment* 787: 147444, doi: 10.1016/j.scitotenv.2021.147444.

Table 1. Chemical and physical properties of the studied topsoils.

Property \ Site	LYR 3	LYR 4	LYR 8
Horizon	A	AC	A
Depth (cm)	0–10	0–10	0–10
pH (H_2O)	5.87	5.92	6.56
SOC (%)	1.63	0.58	2.65
TN (%)	0.17	0.07	0.17
C/N	10	8	15
Rock fragments (%)	60	40	30
Sand (%)	65	46	42
Silt (%)	29	43	47
Clay (%)	6	11	11
Soil texture (USDA)	Sandy loam	Loam	Loam
SiO_2 (%)	69.75	75.99	62.51
Al_2O_3 (%)	11.30	10.11	14.24
Fe_2O_3 (%)	5.99	4.58	6.80
MgO (%)	0.73	0.60	1.06
CaO (%)	0.31	0.22	0.48
Na_2O (%)	1.45	1.46	1.56
K_2O (%)	2.39	2.19	2.48
TiO_2 (%)	0.58	0.59	0.80
P_2O_5 (%)	0.16	0.09	0.16
MnO (%)	0.05	0.05	0.05
Ca^{2+} (cmol/kg)	3.30	2.32	7.85
Mg^{2+} (cmol/kg)	1.83	1.22	2.48
K^{+} (cmol/kg)	0.18	0.09	0.18
Na^{+} (cmol/kg)	0.08	0.07	0.07
H^{+} (cmol/kg)	0.13	0.13	0.09
Al^{3+} (cmol/kg)	1.27	1.36	0.00
K_{av} (mg/100 g)	5.52	2.50	6.14
Mg_{av} (mg/100 g)	38.32	26.72	46.25
P_{av} (mg/100 g)	0.06	1.32	0.38

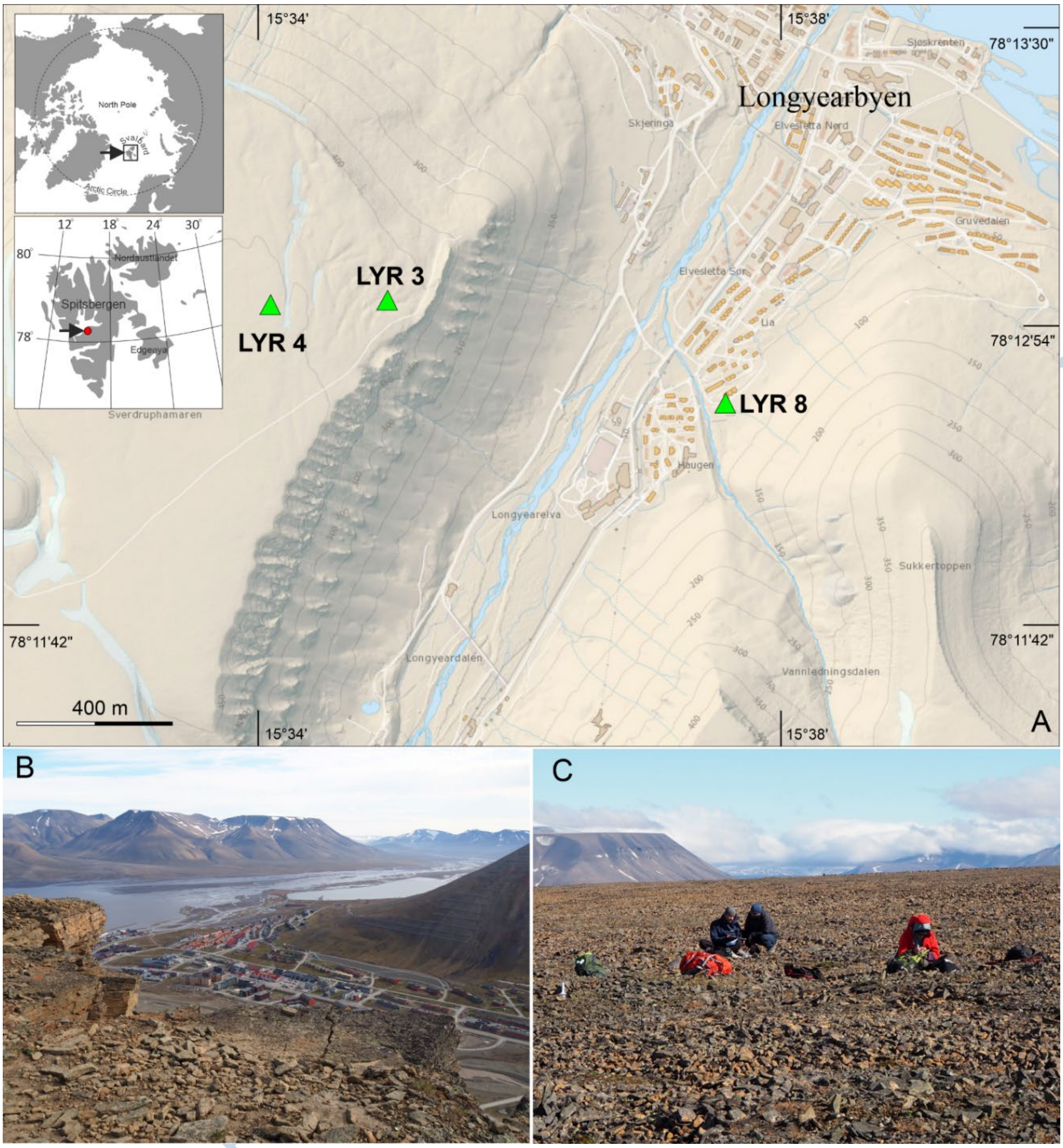

Fig. 1. (**A**) Locations of the research sites in the close vicinity of Longyearbyen in the central part of Spitsbergen, (**B**) general view of Longyearbyen and the lower part of the Longyerelva Valley with location of the LYR 8 site, (**C**) general view of Platåberget covered by loose rock material, where the LYR 3 and LYR 4 research sites were located.

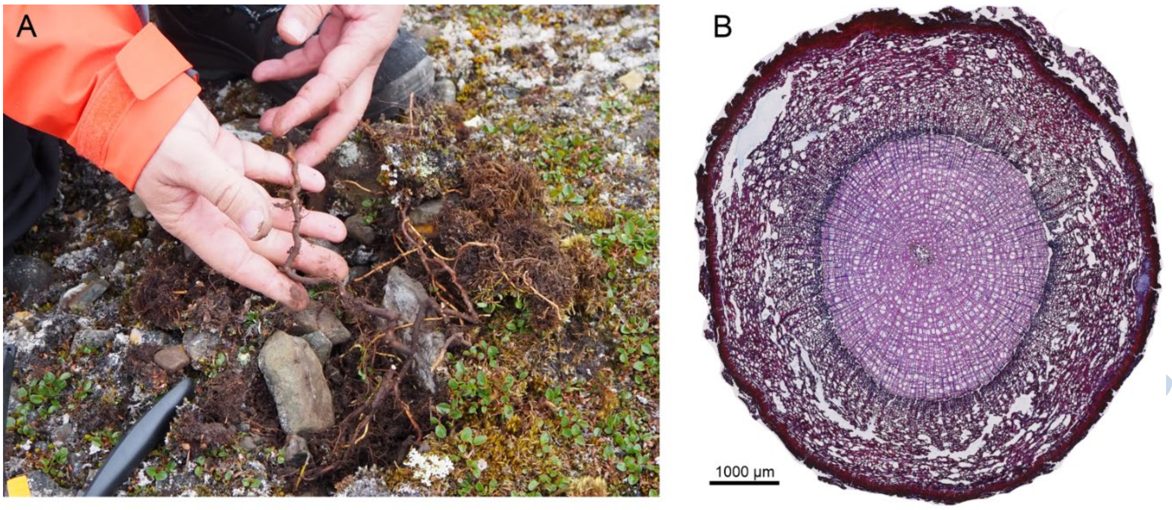

Fig. 2. An example of *Salix polaris* collected for laboratory analysis (**A**), note the long, thick main root and the dense network of thin, woody shoots and (**B**) cross-section through a woody shoot of *Salix polaris*; hick bark accounts for almost 50% of the entire cross-section.

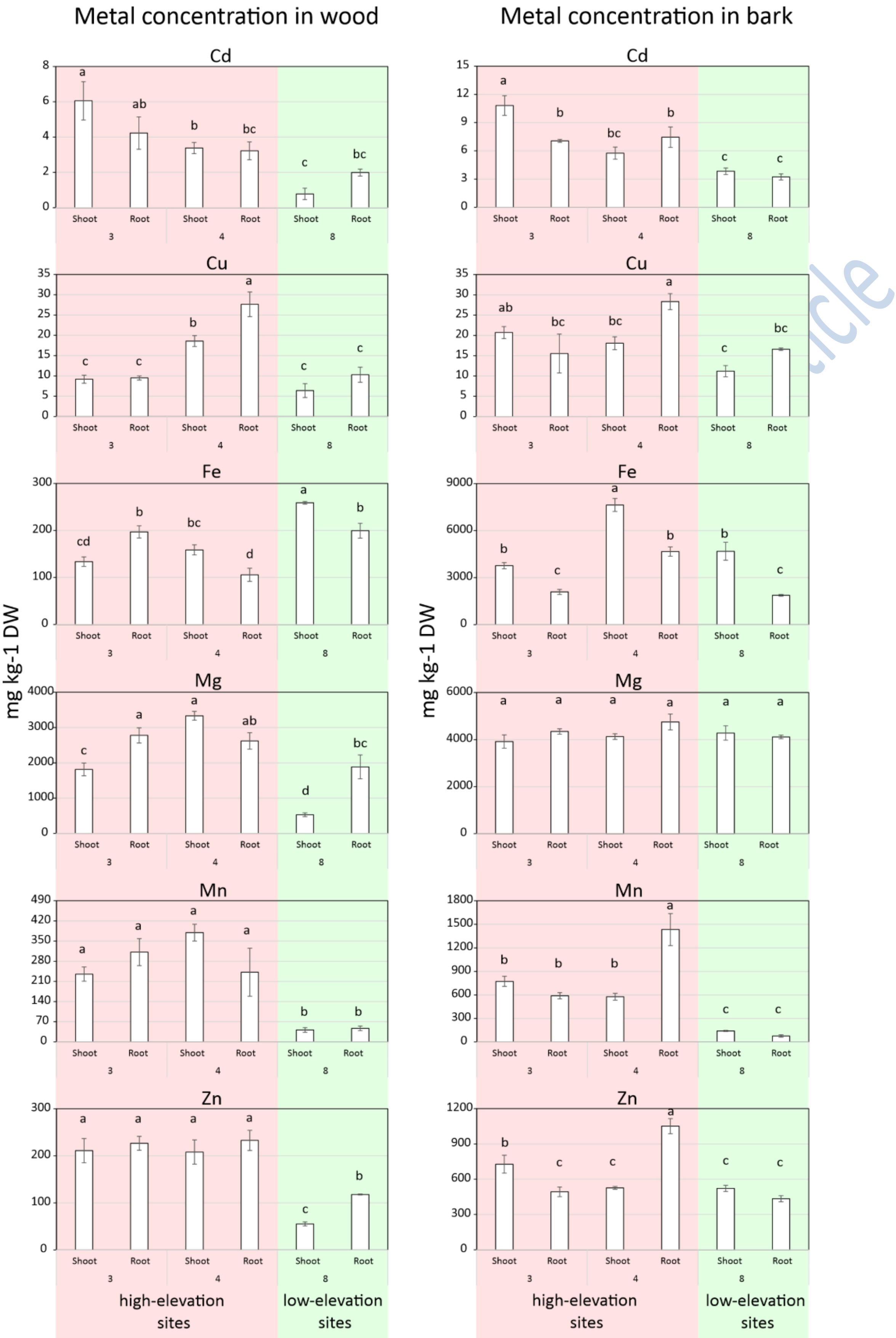

Metal concentration in wood
Metal concentration in bark
Cd
Cu
Fe
Mg
Mn
Zn
mg kg-1 DW
Shoot
Root
3
4
8
high-elevation sites
low-elevation sites

Fig. 3. Metal concentration in wood and bark of wooden shoots and roots in high-elevation research sites LYR 3 and LYR 4 and in low-elevation site LYR 8. Presented data are means ± SE (n = 3). Means followed by the same letter for each metal concentration in *Salix polaris* tissue are not significantly different from each other using the LSD test ($P < 0.05$).

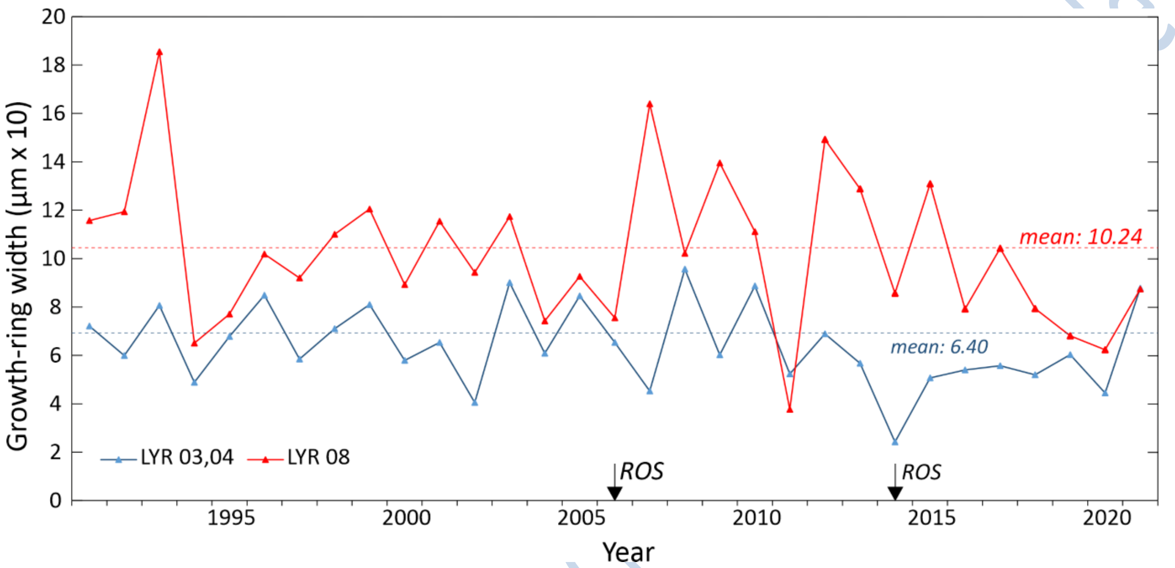

Fig. 4. Growth-ring chronology of *Salix polaris* growing at high (blue line) and low (red line) elevation sites with marked average width of annual increments and rain-on-snow (ROS) events.

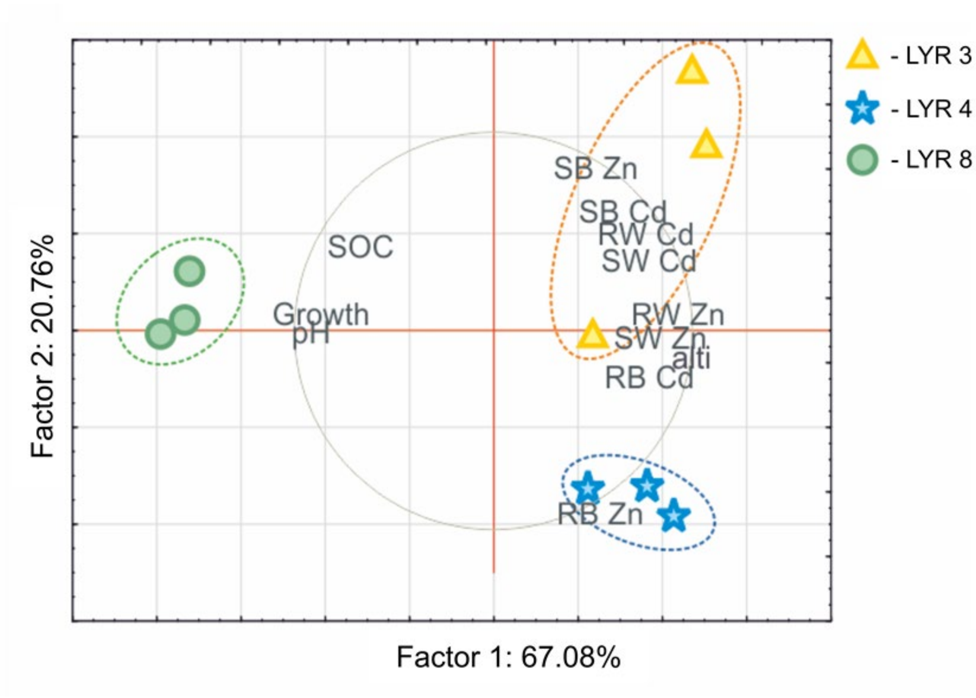

Fig. 5. Principal component analysis presenting the relationships between some environmental factors and heavy metal accumulation in different tissues of *Salix polaris* growing on three sites (LYR 3, LYR 4, LYR 8). Abbreviations: alti – site's altitude, pH – soil pH, SOC – soil organic carbon; Growth – growth-ring width, RB – metal accumulation in root bark, RW – metal accumulation in root wood, SB – metal accumulation in shoot bark, SW – metal accumulation in shoot wood.

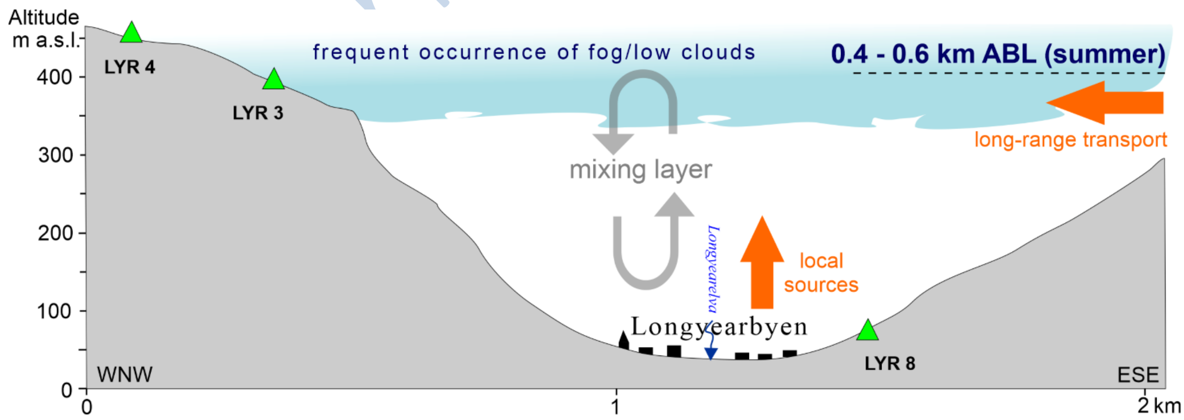

Fig. 6. Cross-section through the Longyerelva valley showing the location of research sites and the height of the Arctic Atmospheric Boundary Layer (ABL) during the summer season.